

## Electronic Supplementary Information

### Atomic layer deposition of Pt nanoparticles onto Co/MoN nanoarrays for improved electrochemical detection of H<sub>2</sub>O<sub>2</sub>

Jinzheng Liu<sup>a</sup>, Xue Li<sup>b</sup>, Lidi Cheng<sup>b</sup>, Junwei Sun<sup>a</sup>, Xiaomin Xia<sup>b</sup>, Xiaoyan Zhang<sup>a</sup>, Yanyan Song<sup>a</sup>, Deshuai Sun<sup>\*a</sup>, Jian Sun<sup>\*b</sup>, and Lixue Zhang<sup>\*a,b</sup>

a. College of Chemistry and Chemical Engineering, Qingdao University, Qingdao 266071, Shandong, P. R. China.

E-mail: zhanglx@qdu.edu, luckysds@qdu.edu.cn

b. The Affiliated Hospital of Qingdao University, School of Stomatology of Qingdao University, Qingdao 266003, P. R. China

E-mail: sunjianqdfy@qdu.edu.cn

## Experimental section

### *Chemicals*

All the chemicals were obtained from commercial suppliers and used without further purification.  $\text{Co}(\text{NO}_3)_2 \cdot 6\text{H}_2\text{O}$ ,  $\text{Na}_2\text{MoO}_4 \cdot 2\text{H}_2\text{O}$ , HCl, benzoic acid and ethanol were bought from Sinopharm Chemical Reagent Corp. (Methylcyclopentadienyl)-trimethyl platinum ( $\text{MeCpPtMe}_3$ ) was purchased from Sigma-Aldrich Chemical Reagent Co., Ltd. Nickel foam (NF) was purchased from Shenzhen Green and Creative Environment Science and Technology Co., Ltd. Deionized water was provided by Ulupure UPR-II-10T system.

### *Preparation of $\text{CoMoO}_4$ on Nickel Foam (NF)*

The synthesis of  $\text{CoMoO}_4$  nanosheet arrays was achieved by hydrothermal reaction and air oxidation. Firstly, 2 cm  $\times$  3 cm NF was treated by ultrasonic treatment for 30 min in HCl (30 wt%), water and ethanol, respectively. 1.5 mM  $\text{Co}(\text{NO}_3)_2 \cdot 6\text{H}_2\text{O}$  and 1.5 mM  $\text{Na}_2\text{MoO}_4 \cdot 2\text{H}_2\text{O}$  were dissolved in 50 mL deionized water under vigorous stirring for 30 min to form a homogeneous solution. The treated NF and the solution were put into a 50 mL stainless steel autoclave and kept at 140 °C for 10 h. The obtained NF was cleaned by ultrasound with ultrapure water and ethanol and dried at 60 °C. Finally, it was oxidized in air at 500 °C for 2 h to obtain  $\text{CoMoO}_4$  nanosheet arrays.

### *Preparation of Co/MoN nanoarrays on NF*

The  $\text{CoMoO}_4/\text{NF}$  was heated to 500 °C in  $\text{NH}_3$  atmosphere and maintained for 2 h, and then naturally cooled to room temperature to form Co/MoN nanosheet arrays.

### *Preparation of Pt@Co/MoN*

The deposition of Pt onto Co/MoN was realized by atomic layer deposition (ALD) technique, which was carried out in a hot-wall, closed chamber-type ALD reactor (D100-4P8C8H2F). The Co/MoN was placed in the ALD chamber and during the reaction process, nitrogen acted as the carrier gas, and  $\text{MeCpPtMe}_3$  acted as precursor of Pt element. The pulse, exposure, and purge times for the precursor was 0.5, 10, and 20 s, respectively, and for ozone, the times was 1, 12, and 25 s, respectively. The typical deposition cycles were 10, 20, and 30.

### *Characterization*

Field emission scanning electron microscope (JSM-7001F, JEOL, Tokyo, Japan) and

transmission electron microscope (FEI Tecnai F20, America) were used to characterize the morphologies and structures of all the samples. Powder X-ray diffraction data was obtained from a SmartLab3KW X-ray Diffractometer (Rigaku Corporation, Japan) for the crystal structural characterization. X-ray photoelectron spectroscopy experiments were performed on an Axis Supra+ X-ray photoelectron spectrometer (Shimadzu Corporation, Japan). Inductively coupled plasma mass spectrometry (ICP-MS) analysis was performed on Agilent 7800 (America). Fluorescent detection experiments were performed on F-7000 fluorescence spectrophotometer (Hitachi, Japan).

### *Electrochemical Tests*

Electrochemical tests were performed using the CHI730 Electrochemical Workstation in 0.01 M phosphate buffered saline (PBS, pH=7.4) solution in oxygen-depleted N<sub>2</sub> saturated atmosphere. Co/MoN/NF or Pt@Co/MoN/NF were cut into 0.3 cm×0.4 cm pieces and clamped on the electrode as the working electrode. Ag/AgCl and Pt wires were used as reference and counter electrode, respectively. For the detection of H<sub>2</sub>O<sub>2</sub> in milk and orange juice, the sample milk (New Hope Pure Milk) and orange juice (Nongfu Spring NFC) were diluted by 20 times with 0.01 M PBS (pH=7.4), and 10 μM H<sub>2</sub>O<sub>2</sub> was sequentially added to the test solution.

### *Electrochemical Detection of H<sub>2</sub>O<sub>2</sub> Released from Cells*

The original RAW 264.7 cells were cultured in 5% CO<sub>2</sub> in a 50 cm<sup>2</sup> flask containing Dulbecco's modified Eagle medium containing 1% antibiotics and 10% (v/v) fetal bovine serum at 37 °C. Cells were separated from culture medium by 5 min of centrifugation at 5000 rpm and washed for three times with the physiological PBS (0.01 M, pH=7.4) solution. Cell number was estimated by a cell counter. When the current keeps stable, 3-[(3-Cholamidopropyl) dimethylammonio]-1-propanesulfonate (CHAPS) was injected to the cell suspension, which can motivate cells generation of H<sub>2</sub>O<sub>2</sub> and have no interference to the detection of H<sub>2</sub>O<sub>2</sub>. The amperometric current response of H<sub>2</sub>O<sub>2</sub> in about 2.0×10<sup>7</sup> cells in 17 mL of deoxygenated PBS on the Pt@Co/MoN-20 electrode was recorded at -0.25 V (vs. Ag/AgCl). The experiments were conducted at the room temperature (25 °C).

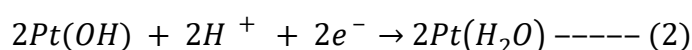
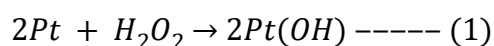
### *Detection of hydroxyl radicals by fluorescence spectroscopy*

Benzoic acid was used as the fluorescence probe to determine the formation of hydroxyl radicals in the reaction process. The electrolyte was 0.01M PBS (pH=7.4)

solution containing 1 mM H<sub>2</sub>O<sub>2</sub> and 5 mM benzoic acid. The dilutions before the electrochemical reaction, and after electrochemical reaction for 15min, 30min and 1 h at -0.25V (vs. Ag/AgCl) were taken for fluorescent experiments. The excitation wavelength of all the fluorescence tests was 320 nm.

#### *Mechanism of H<sub>2</sub>O<sub>2</sub> reduction reaction on Pt*

The electrochemical reduction reaction of H<sub>2</sub>O<sub>2</sub> on Pt in a neutral solution (pH = 7.4) is proposed to follow the following steps [1-3].



Firstly, at an adequately low potential, H<sub>2</sub>O<sub>2</sub> dissociates into two hydroxyl radicals on Pt active sites via a non-electrochemical manner (Step 1). The generated hydroxyl radicals mostly remain adsorbed on the surface of Pt (denoted as OH<sub>ads</sub>) and partially may be released into the solution to form free ·OH [4]. Then, because of the instability of the adsorbed OH<sub>ads</sub>, it easily undergoes an electrochemical reduction with proton and electron to form H<sub>2</sub>O (Step 2), and simultaneously the Pt active sites re-generate and can be used to dissociate other H<sub>2</sub>O<sub>2</sub> molecules again.

To identify the possible existence of free hydroxyl radicals, a fluorescent experiment was conducted by using benzoic acid as the fluorescence probe, which can react with hydroxyl radical to produce hydroxybenzoic acid with a strong fluorescence signal [5]. As shown in the Fig. S8, after an electrocatalytic reduction of H<sub>2</sub>O<sub>2</sub>, the characteristic peak of hydroxybenzoic acid appeared and increased with the duration of reaction, confirming the existence of free hydroxyl radicals during the electrochemical process.

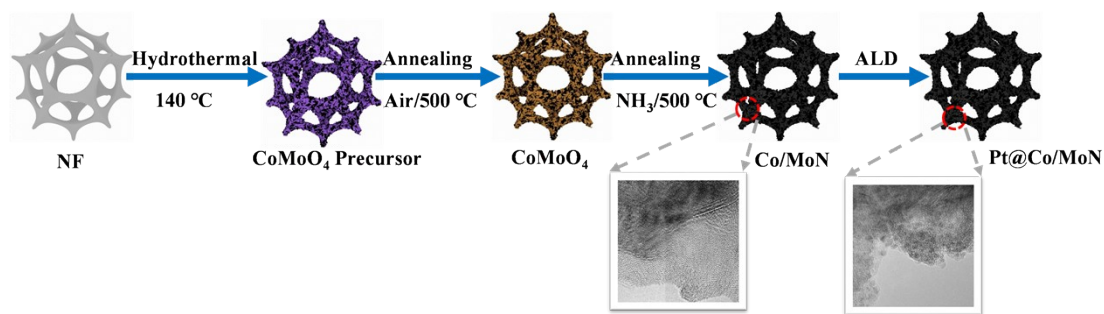


**Fig. S1** Schematic diagram of the preparation of the Pt@Co/MoN sensing platform.

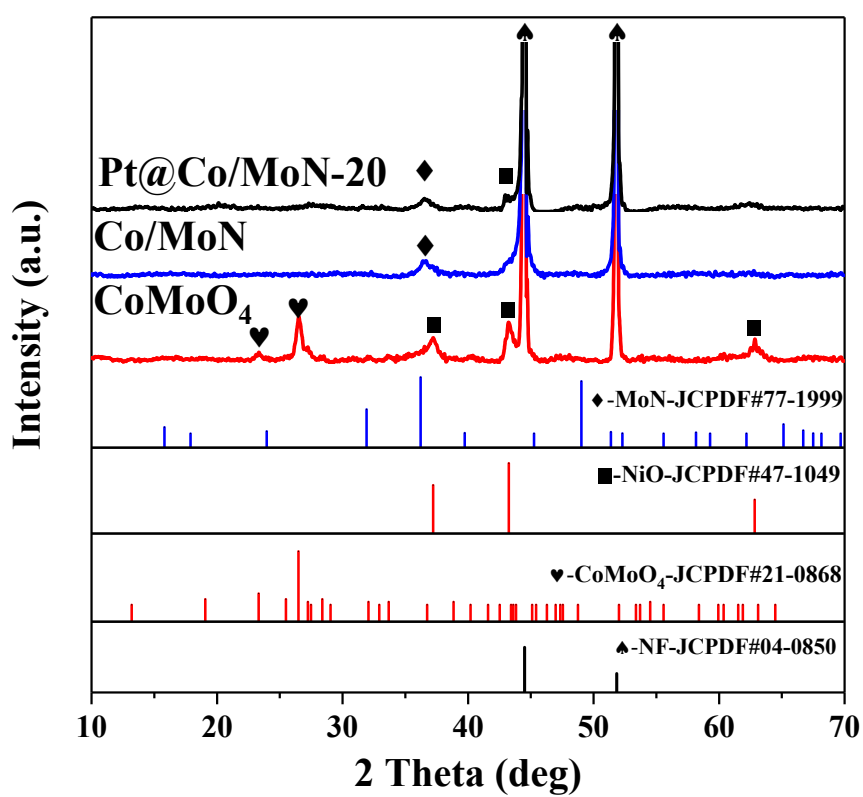


**Fig. S2** XRD patterns of CoMoO<sub>4</sub>, Co/MoN and Pt@Co/MoN-20.

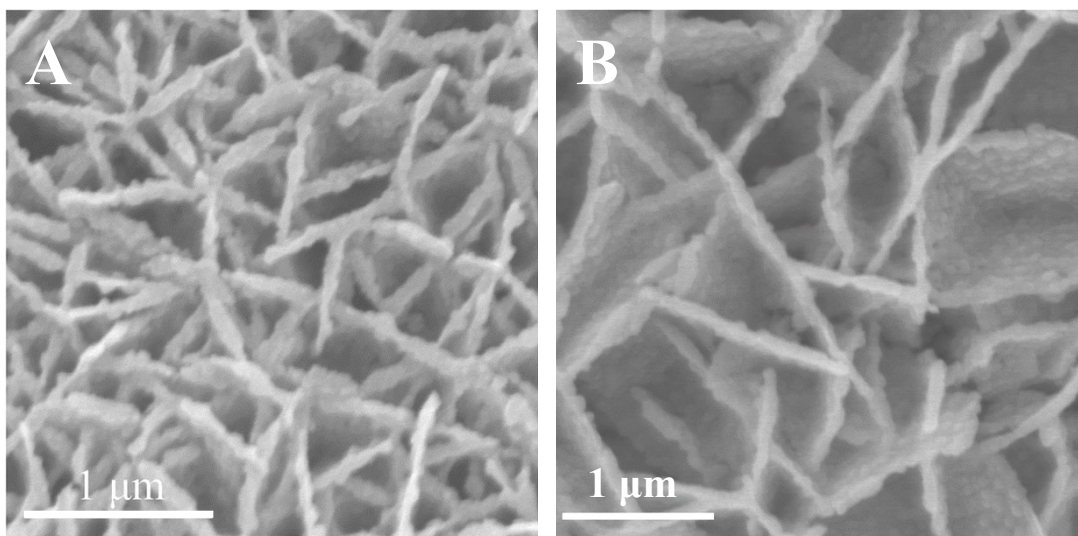


**Fig. S3** (A) SEM image of Co/MoN nanosheet array. (B) SEM image of Pt@Co/MoN-20 nanosheet array.

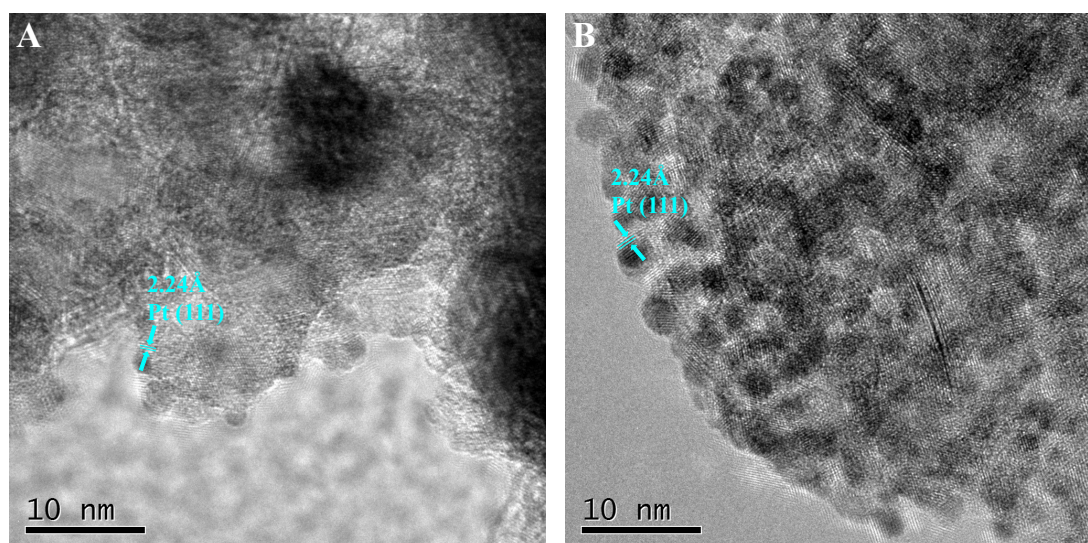


**Fig. S4** (A) High resolution TEM image of Pt@Co/MoN-10. (B) High resolution TEM image of Pt@Co/MoN-30.

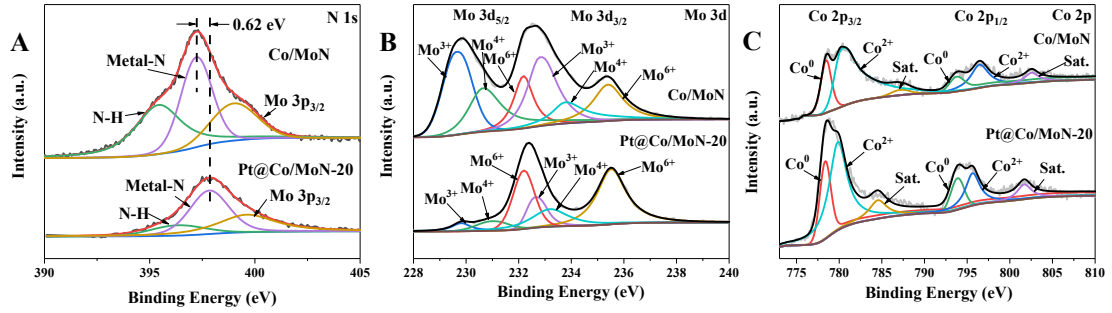


**Fig.S5** The high resolution XPS spectra for N 1s (A), Mo 3d (B), and Co 2p (C) of Pt@Co/MoN-20 and Co/MoN.

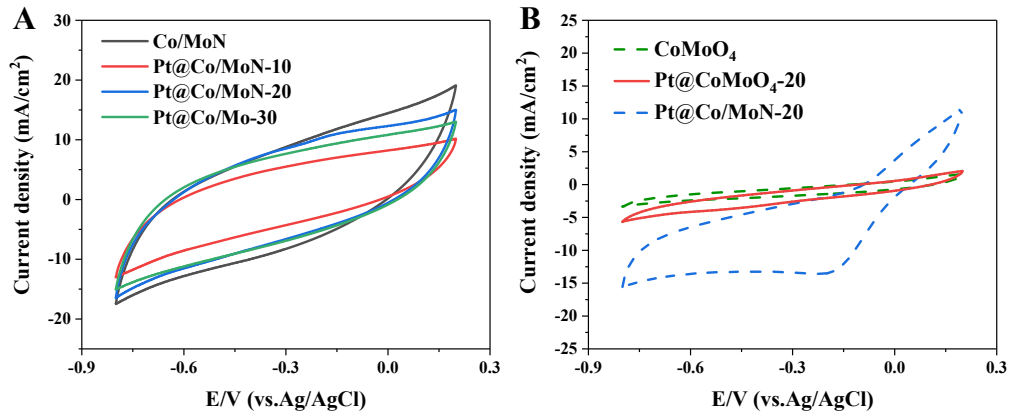


**Fig. S6** (A) CV curves of the prepared electrodes in 0.01 M PBS (pH=7.4) at a scan rate of 50 mV s<sup>-1</sup>. (B) CV curves of CoMoO<sub>4</sub>, Pt@CoMoO<sub>4</sub>-20 and Pt@Co/MoN-20 in 0.01 M PBS (pH=7.4) with the presence of 5 mM H<sub>2</sub>O<sub>2</sub> at a scan rate of 50 mV s<sup>-1</sup>.

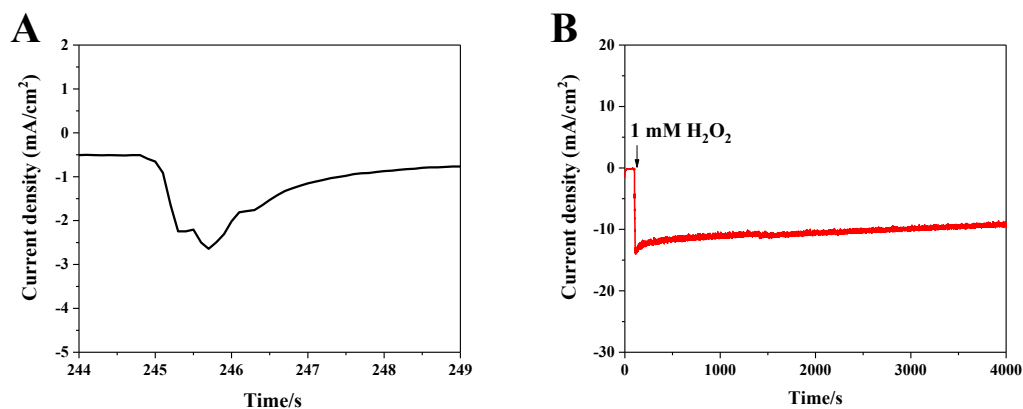


**Fig. S7** (A) I-t curve of Pt@Co/MoN-20 at -0.25 V (vs.Ag/AgCl) potential in the 0.01M PBS (pH=7.4) towards 1.8  $\mu$ M  $H_2O_2$ . (B) I-t curve of Pt@Co/MoN-20 toward 1 mM  $H_2O_2$  at -0.25 V (vs.Ag/AgCl) for 3800 s.

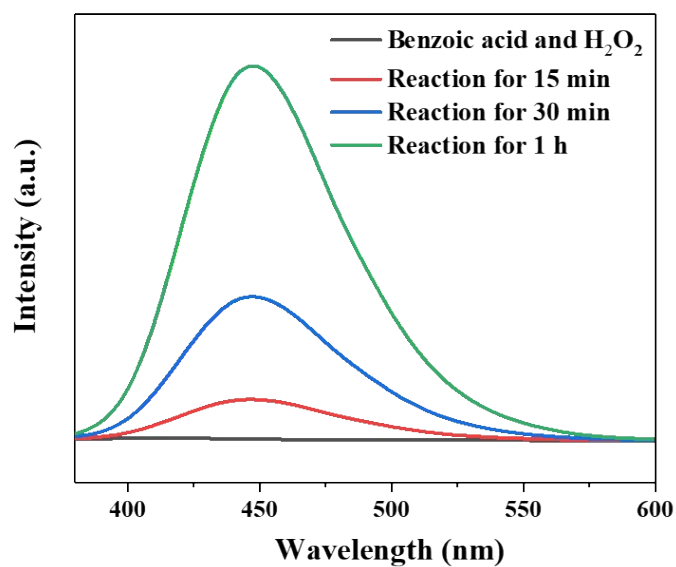


**Fig. S8** Fluorescence spectra of the hydroxyl radicals detection in the solution after different electrochemical reduction intervals using benzoic acid as indicator (excitation wavelength=320nm).



**Table S1** Comparison of analytical features of the Pt@Co/MoN-20 sensing platform and other nano Pt-based sensing platforms for the electrochemical detection of hydrogen peroxide.

<b>Electrode materials</b>	<b>Linear response (<math>\mu\text{M}</math>)</b>	<b>LOD (<math>\mu\text{M}</math>)</b>	<b>Reference</b>
Pt NPs/CFEs	0.5–80	0.17	6
4 nm PtNPs/GCE	25–750	10	7
Pt <sub>20</sub> @SNM/ITO	10–5000	10	8
MoS <sub>2</sub> /Pt	1-100	0.686	9
Pt-Pd/MoS <sub>2</sub>	10-80	3.4	10
Au@Pt NPs/ITO	0.5-1000	0.11	11
PtSPE/ZnONPs/GA/GGP	100–2250	84	12
<b>Pt@Co/MoN-20</b>	<b>0.6-979</b>	<b>0.313</b>	<b>This work</b>

**Table S2** The electrochemical detection of Pt@Co/MoN-20 compare to the spectroscopic detection of H<sub>2</sub>O<sub>2</sub>.

<b>Catalysts</b>	<b>Detection method</b>	<b>LOD (μM)</b>	<b>Linear response (μM)</b>	<b>Reference</b>
Carbon dots-doped CeO <sub>2</sub> (CeO <sub>2</sub> -CDs)	UV-vis	0.35	1.67 - 2010	13
Polyacrylonitrile-copper oxide (PAN-CuO)	UV-vis	0.12	0.5 - 125	14
g-C <sub>3</sub> N <sub>4</sub> NSs-Ce <sup>3+</sup> -CuNCs	FS	0.6	2-100	15
Mito-FBN	FS	0.025	1-60	16
MoS <sub>2</sub> QDNS	PL	2	2-94	17
AgInS <sub>2</sub> quantum dots (AIS QDs)	PL	0.42	0.5-300	18
<b>Pt@Co/MoN-20</b>	<b>Electrochemical method</b>	<b>0.313</b>	<b>0.6-979</b>	<b>This work</b>

## References:

- 1 R. Serra-Maia, M. Bellier, S. Chastka, K. Tranhuu, A. Subowo, J. D. Rimstidt, P. M. Usov, A. J. Morris, F. M. Michel, *ACS Appl. Mater. Interfaces*, 2018, 10, 21224–21234.
- 2 Y. Liu, H. Wu, M. Li, J. Yin, Z. Nie, *Nanoscale*, 2014, 6, 11904.
- 3 I. Katsounaros, W. B. Schneider, J. C. Meier, U. Benedikt, P. U. Biedermann, A. A. Auer, K. J. J. Mayrhofer, *Phys. Chem. Chem. Phys.*, 2012, 14, 7384–7391.
- 4 L. Luo, W. Chen, S. Xu, J. Yang, M. Li, H. Zhou, M. Xu, M. Shao, X. Kong, Z. Li, H. Duan, *J. Am. Chem. Soc.*, 2022, 144, 7720–7730.
- 5 B. Gao, Y. Pan, H. Yang, *Appl. Catal. B-Environ.*, 2022, 315, 121580.
- 6 Y. Tong, L. Wang, J. Song, M. Zhang, H. Qi, S. Ding, H. Qi, *Anal. Chem.*, 2021, 93, 16683–16689.
- 7 E. Mazzotta, T.D. Giulio, V. Mastronardi, P. P. Pompa, M. Moglianetti, C. Malitesta, *ACS Appl. Nano Mater.*, 2021, 4, 7650–7662.
- 8 X. Li, L. Zhou, J. Ding, L. Sun, B. Su, *ChemElectroChem*, 2020, 7, 2081–2086
- 9 J. Zhou, L. Tang, F. Yang, F. Liang, H. Wang, Y. Li, G. Zhang, *Analyst*, 2017, 142, 4322.
- 10 R. Sha, N. Vishnu, S. Badhulika, *Microchim. Acta*, 2018, 185, 399.
- 11 C. Xia, W. He, X. Yang, P. Gao, S. Zhen, Y. Li, C. Huang, *Anal. Chem.*, 2022, 94, 13440–13446.
- 12 P. A. Uribe, C. C. Ortiz, D. A. Centeno, J. J. Castillo, S. I. Blanco, J. A. Gutierrez, *Colloids Surf. A*, 2019, 561, 18–24.
- 13 Z. Yang, Y. Liu, C. Lu, G. Yue, Y. Wang, H. Rao, W. Zhang, Z. Lu, X. Wang, *J. Alloy. Compd.*, 2021, 862, 158323.
- 14 X. Zheng, Q. Lian, L. Zhou, Y. Jiang, J. Gao, *ACS Sustain. Chem. Eng.*, 2021, 9, 7030–7043.
- 15 H. Mei, Q. Wang, J. Jiang, X. Zhu, H. Wang, S. Qu, X. Wang, *Talanta*, 2022, 248, 123604.
- 16 J. Liu, J. Liang, C. Wu, Y. Zhao, *Anal. Chem.*, 2019, 91, 6902–6909.
- 17 N.P. Mani, J. Cyriac, *Anal. Bioanal. Chem.*, 2019, 411, 5481–5488.
- 18 L. Wang, X. Kang, D. Pan, *Inorg. Chem.*, 2017, 56, 6122–6130.